SOLAR ENERGY FOR OPTIMIZED CONTROLLER BASED DC-DC CONVERTER

Abstract

This proposed system presents the management and control of power flow to DC loads in grid-tied photovoltaic systems. Due to its intermittent nature, the PV produces low voltage. Therefore, in order for obtaining substantial power from a solar panel during oscillations in ambient conditions, a DC-DC landsman converter is used in this study. In addition to this, the ripples in the output voltage and settling time are reduced. For the efficient use of the DC distribution system (DCDS) and for the power grid to remain stable, the Spotted Hyena Optimized (SPO) PI controller with DC-DC converter is employed. Where the controller's parameters, which take into account the total of the errors of the reference and output voltage are optimized. The PWM generator receives the controller's output and produces the PWM pulses required for the Landsman converter to operate properly. The grid is then given the continuous DC link voltage. By simulating and running the suggested system's simulation model in MATLAB, the proposed converters and the controller's veracity is examined. It is proven from the deduced data that the suggested system performs at 96% efficiency with a low Total Harmonic Distortion of 2.32%.

Keywords: PV system, Landsman DC-DC Converter, Spotted Hyena Optimized PI controller, PWM generator, Grid.

Authors

Siddheshwar Kar
Assistant Professor
Department of Electrical Engineering,
Medi-Caps University
Madhya Pradesh, India.
India.siddheshwarkar1@gmail.com

Riyaz A Rahiman
Associate Professor
School of Electronics and Communication
Reva University
Bangalore, Karnataka, India.

S. L. Sreedevi
Assistant Professor
Department of Electrical and Electronics Engineering, PERI Institute of Technology
Chennai, India.

Sharda Patwa
Assistant Professor
Department of Electrical Engineering
Medi-Caps University
Madhya Pradesh, India.

I. INTRODUCTION

Renewable energy use is growing globally and is gaining traction in distribution networks. This is due to a variety of issues, including expanding energy usage, dwindling availability of conventional fuels, and growing environmental concerns. Due to the rising efficiency and falling cost of production, photovoltaic (PV) power sources are swiftly overtaking other renewable energy sources as the most promising source of electricity. But the key problems with the deployment of PV in the real world are the solar cell's high climatic sensitivity and extremely limited primary energy conversion efficiency [1]. To address these issues, DC-DC converters were used with the subsequent synthesis of control systems. Various non-isolated DC-DC converters are used for photovoltaic applications. The traditional boost converter [2] is widely used and makes it is challenging to use in real-world applications because of high switching voltage stress and problems with reverse recovery issues. The cuk and SEPIC converter [3] has nearly the same characteristics as the characteristics of the Buck-Boost Converter. The buck-boost converter [4] has been shown to be the greatest alternative among the many non-isolated DC-DC converters since it offers an unlimited zone for MPPT. For the desired operation of the complete system, a buck-boost converter, on the contrary hand, always needs a ripple filter for both its output and input, leading to corresponding circuitry. The flaws of numerous previously used converters in SPV array are all resolved by this work's adaptation of a Landsman converter. In this converter, external ripple filtering is not required because the small input inductor serves as an input-ripple filter. Additionally, this inductor reduces oscillations in the module's current flow brought on by the insulated gate bipolar transistor (IGBT) module's rejected components. By using Landsman converter, the voltage gets improved which in turn to maintain stability, control algorithms are required.

Various Standard control methods and optimization-based controllers were employed for optimal determination of controller attributes due to voltage variations. The well recognized analytical methods such as Hill-climbing (HC), incremental conductance, perturb and observe algorithm exhibit amazing qualities like reduced complexity, simple implementation and effective tracking at zero shadow. However, it is prone to steady-state oscillations and inefficiency under Partial shading circumstances [5], [6]. As an alternate strategy, fuzzy logic control (FLC) and artificial neural network (ANN) are used. However, the requirement for period training and the significant computing cost limit its use [7], [8]. In current scenario, metaheuristic-based approaches are gaining high attention due to the property that it is not problem dependent and the ability to avoid the local minima trap, is an advantage of the heuristic method over the deterministic method. The deterministic one, on the other hand, is slower in nature. In current scenario, several metaheuristic [9], [10] based controllers were used to tune the control parameter. The trade-off between exploration and extraction is the most important aspect influencing the performance and accuracy of a metaheuristic algorithm. The Spotted Hyena optimization-based controller, which makes a good trade-off between the exploitation and exploration stages and produces the optimized results.

Solar energy is mostly utilized in this system's intended power supply for the grid. The Landsman converter, which makes up a large portion of the system, is utilized to increase the power efficiency of PV. The DC-DC converter enhances the voltage gain to the desired limit. Which in turn, the outcome from the converter is led into the Spotted hyena

optimized PI controller where the parameters of the controller are optimized that that evaluates the suitability of each solution using the sum of the errors between the reference voltage and the output voltage as well as the errors among the values of the inductor current at every single switch opening moment. This controller is employed due to the algorithm being used to its full potential, improved accuracy is the first and foremost benefit. This also leads to optimized parameters. The second benefit is that because of its high exploration, it can successfully avoid local minima problems. The third benefit is its convergence speed: even though it is showing extremely promising accuracy performance, its convergence rate is also quite rapid.

II. RELATED WORKS

Jaime et al [11] explains how well two-stage solar energy systems perform at the dc-dc stage. This paper analyzed several Partial Power Converter Topologies (PPC) and connection combinations. The examined topologies and combinations show that the Partial Power Converter idea is flexible enough to be applied to step-down dc-stages for bigger PV strings or step-up dc-stages for micro inverters and small PV strings. The results show that the MPPT performance can still be maintained even though the converter is only able to process a tiny percentage of the power. The PPC connection also offers new advantages including reduced input current ripple that can lengthen the capacitors' lives. But because the switching states of the converter remain standalone, PPCs cannot be used to balance out imbalances between parts that are coupled in series.

Rui Li et al [12] discuss the isolated bidirectional DC-DC converter with high efficiency. In this system, the two-stage isolated converter is employed that uses two inductors and capacitors (LLC) or capacitor-inductor-inductor-capacitor (CLLC) to offer greater DC gain and electrical isolation. In addition to this, Bi-directional DC to DC converters provide more flexibility in power management and distribution. They allow power transfer in either direction as required by connecting various DC voltage sources with various voltage levels. However, it is not widely used in high power applications because bidirectional DC-DC converters require complicated control systems to manage power flow in both directions, which can increase system complexity, cost and stability problems with regard to managing power flow and regulating voltage.

Pierre et al [13] explains the application of a phase-shifted full bridge (PSFB) converter in moderate-voltage dc collection networks for solar power stations. Zero-voltage switching (ZVS) is possible with a FULL-BRIDGE converter that uses phase-shifted control refrain from the necessity of supplementary components. Excellent productivity and elevated power density are the phase-shifted full-bridge (PSFB) converter's main attributes, making them ideal for midrange and powerful uses. Under low load circumstances, on the other hand, the Zero Voltage Switching property fades away, leading to decreased performance and considerable electromagnetic interference. Additionally, the existence of flowing current while in the freewheeling interval significantly raises conduction loss.

Ali et al [14] explains a new Bat Algorithm Strategy for MPPT in Photovoltaic Energy Systems with Dynamic Partial Shading. The proposed bat technique obtains the greatest results in terms of continuously monitoring the GP in conditions of sudden shifts in partial shading. The Bat Algorithm (BA) is used to track the global peak (GP) of PV power

sources because of its speedy convergence. When employed as a PV system's maximum power point tracker (MPPT), BA has a number of drawbacks, including the challenge of early convergence and the requirement for re-initialization.

Moustafa et al [15] established a novel way for integrating global Maximum Power Point tracking with Output Voltage Regulation (OVR) control for partially shaded PV modules. Compared to other controllers, the number of sensors used in this system is low which results in associated size, cost, and measurement losses. Additionally, the designed output voltage regulation mechanism aims to lower converter electrical losses via efficient PV operating point allocation. However, when there is a significant disparity between the input and output voltages, the productivity is unsatisfactory.

III. PROPOSED SYSTEM

1. **Proposed System Description:** Figure 1 shows the suggested system configuration. In this system, the PV supplies energy to the grid through the converter and the subsequent synthesis of PI controller. A DC-DC Landsman converter's significant role is to improve the energy output of a photovoltaic panel and removes the oscillations in the PV output. To maintain the output voltage in a stable mode, controller is required. The spotted hyena optimized PI controller is utilized to establish the proper PI controller parameters with the goal to enhance the converter's dynamics.

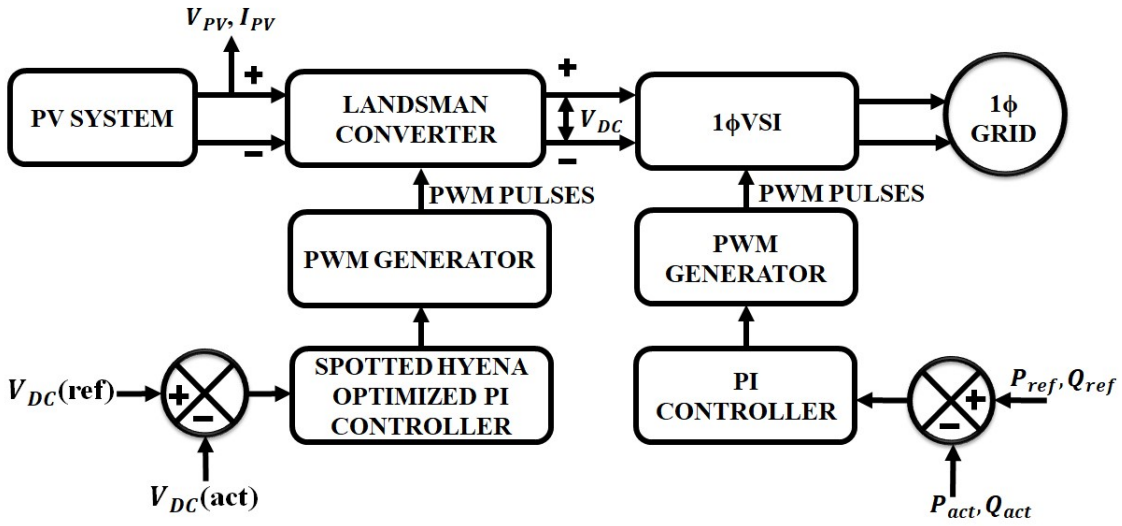

Figure 1: Proposed Block Diagram

The spotted Hyena optimized PI controller compares the actual and reference voltage along with the production of error signal. This error signal is taken into account as an input by the PI controller, which adjusts theK_p and K_i gains. The PWM Generator receives the output from the PI Controller and generates necessary PWM pulses for running the converter. The output voltage from the converter is given to the single -phase Voltage Source Inverter (VSI) that converts DC to AC voltage and then it is fed to the 1φ utility grid.

2. **Modeling of PV:** PV, which transforms solar energy into DC electricity, is the main source used in the proposed work. The PV panel contains a large number of cells, which are arranged in shunt R_{sh} or R_s series. In accordance with shunt and series resistors, a current source is shown in Figure 2 coupled in parallel with a diode.
In equation 1, the output current is given as,

$$I = I_{ph} - I_D \quad (1)$$

$$I = I_{ph} - I_o\left[\exp\left(\frac{q(V+R_sI)}{AK_BT}\right) - 1\right] - \frac{V+R_sI}{R_{sh}} \quad (2)$$

Where, I is the cell current, I_o- saturation current, K_B- Boltzmann's constant, R_S and R_{sh} are the series and shunt resistance respectively.
The optimal voltage-current characteristic for a solar cell is given by,

$$I = I_{ph} - I_o[e^{\left(\frac{qV}{KT}\right)} - 1] \quad (3)$$

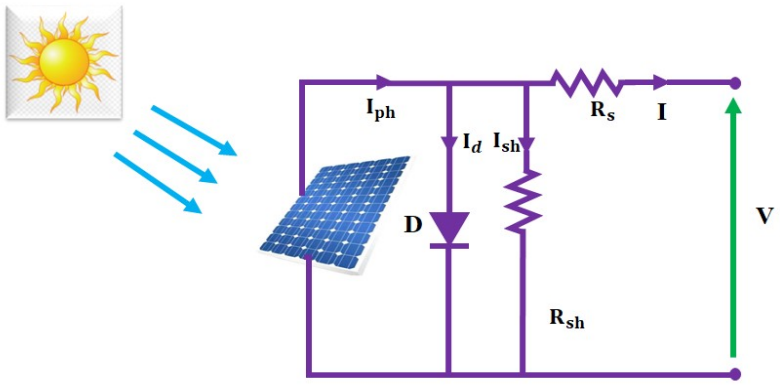

Figure 2: Circuit Diagram of PV Array

Due to the ambient condition, the voltage produced from PV is relatively low. Thus, a DC-DC converter is necessary to boost the voltage. Hence in this system, Landsman converter is used.

3. **Landsman Converter:** To reduce both voltage and current load on the power semiconductor device, the Landsman converter has been optimized to operate in continuous conduction mode (CCM). The Landsman DC-DC Converter circuit diagram and functioning are examined in Figures 3a and 3b.

IV. MODES OF OPERATION

Mode 1: Switch ON

While the switch is activated, energy from the supply and energy that has been stored in the intermediate capacitor(C_1) are transferred to the input inductor(L_i). The DC-link voltage (V_{dc}) begins to rise as the output inductor(L_o) begins to release while the voltage of intermediate capacitor(V_{C1}) begins to decrease. The intermediate capacitor's value is

sufficient to store the necessary energy without causing a discontinuity in the voltage across the capacitor. The functioning of switch ON mode of the Landsman converter is shown below,

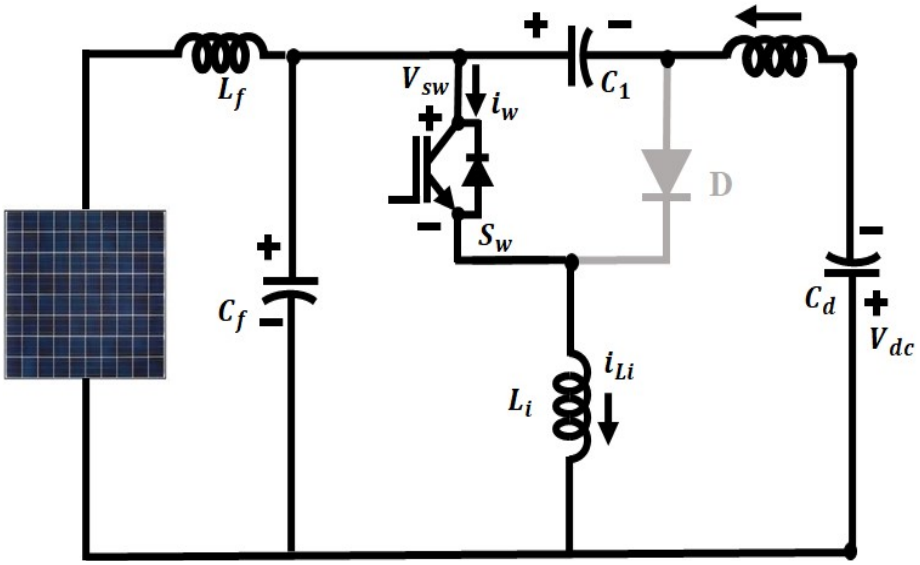

Figure 3: A Circuit of Mode 1

Mode 2: Switch OFF

When the converter is in this mode, the switch is not in the on position. Through the supply current, an intermediate capacitor (C_1) and DC-link side inductor (L_o) are being charged, while output inductor $(L_i)$is starting to be discharged. As a result,V_{C1} starts to rise in this mode. In addition, the voltage (V_{dc}) across the DC capacitor drops.

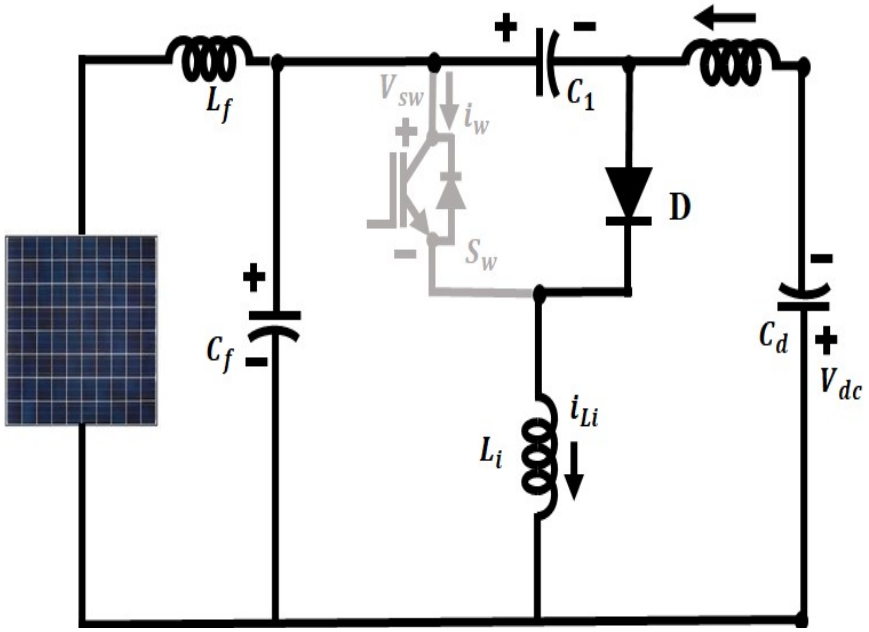

Figure 3: b Circuit of Mode 2

1. **Landsman Converter's Mathematical Model:** The peak-to-peak ripple current ΔIL_1 is given as,

$$\Delta I_{L1} = \frac{\Delta \Phi}{L_1} = \frac{1}{L_1}\frac{1}{2}\frac{\Delta V_{C1}}{2}\frac{T}{2} \qquad (4)$$

During switch OFF mode, the current through C_1 is expressed as,

$$i_{C1} = I_{L1} = C_1 \frac{\Delta V_{C1}}{(1-D)T} \qquad (5)$$

Where T- switching time and D is the duty ratio. The Equation 5 is used to calculate the voltage ripple contentV_{C1} as follows:

$$\Delta V_{C1} = \frac{IL_1}{C_1}(1-D)T \qquad (6)$$

By substituting the equation (6) in (4) gives

$$\Delta IL_1 = \frac{1}{L_1}\frac{1}{2}\frac{IL_1}{2C_1}(1-D)T \qquad (7)$$

$$\Delta I_{L1} = \frac{1}{8L_1C_1}\frac{(1-D)}{f^2 sw} \qquad (8)$$

It is normalized as

$$\frac{\Delta IL_1}{IL_1} = \frac{1}{8L_1}\frac{(1-D)}{f^2 sw} \qquad (9)$$

Where switching frequency$f_{sw} = 1/T$. The bond between input and output makes it obvious that

$$I_{L1} = I_{dc}\frac{D}{1-D} \qquad (10)$$

Where I_{dc}reflects the Landsman converter's output DC current.
By replacing the equation (10) into equation (8), it gives,

$$L_1 = \frac{(DI_{dc})}{8f^2 swC_1 \Delta IL_1} \qquad (11)$$

The Landsman converter offers output voltage that has little ripple content, is very efficient, and has great voltage regulation. In comparison to other DC-DC converters, it is frequently preferred.

2. **Spotted Hyena Optimizer:** SHO uses spotted hyenas' natural hunting strategies as a model while attempting to solve optimization problems. Three distinct behaviors are used to categories the organized group hunting behavior of a pack of spotted hyenas. The behaviors are categorized as Searching or encircling prey, Hunting and attacking.

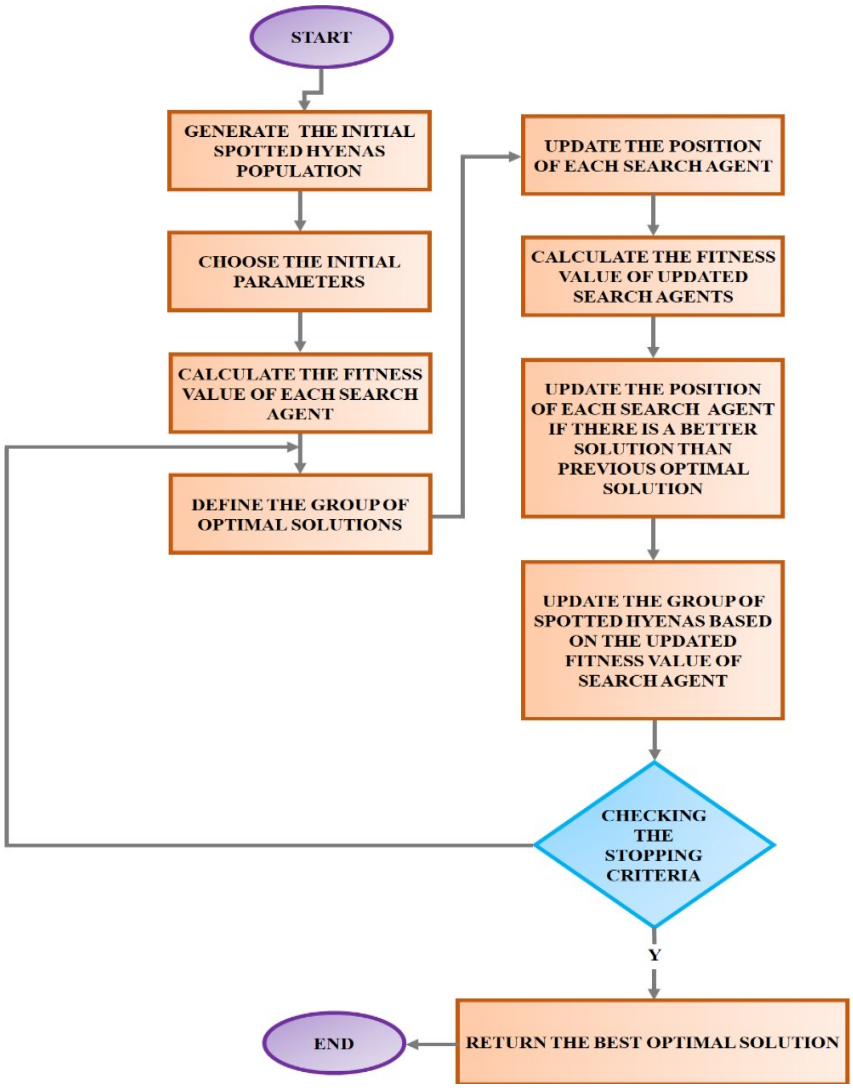

Figure 4: Flowchart of SHO

Equation below produces the mathematical representation of encircling the prey,

$$\vec{D} = |\vec{B}.\vec{X}_P(t) - \vec{X}(t)| \quad (12)$$

$$\vec{X}(t+1) = \vec{X}_p(t) - \vec{E}.\vec{D} \quad (13)$$

Here, the vector coefficients are$\vec{B}, \vec{E}$, current iteration is t and $\vec{X}_p$ - position vector of the prey and $\vec{X}$- position vector correspondingly.

The coefficient vectors are expressed as,

$$\vec{B} = 2.r\vec{d_1} \quad (14)$$

$$\vec{E} = 2\vec{h}.r\vec{d}_2 - \vec{h} \quad (15)$$

$\vec{h}$ is computed in equation (16) which linearly reduces from 5 to 0.

$$\vec{h} = 5 - (t * \left(\frac{5}{T}\right)) \quad (16)$$

To balance exploitation and exploration, t=1, 2, 3, T is employed.

To quantitatively define spotted hyena behavior, the prey's whereabouts is reflected in the ideal search agent. With the goal to keep track of their whereabouts, the remaining search teams copy the best search agent's findings and save the top solutions found thus far. The mathematical representation is as follows:

$$\vec{D}_h = \left|\vec{B}.\vec{X}_h - \vec{X}_k\right| \quad (17)$$

$$\vec{X}_k = \vec{X}_h - \vec{E}.\vec{D}_h \quad (18)$$

The cluster of N optimal solution is given by

$$\overrightarrow{C_h} = \vec{X}_k + \vec{X}_{k+1} + \cdots + \vec{X}_{k+N} \quad (19)$$

$$N = count_{nos}(\vec{X}_h, \vec{X}_{h+1}, \vec{X}_{h+2}, \ldots, (\vec{X}_h + M)) \quad (20)$$

It is required to repeatedly decrease the amount of $\overrightarrow{h}$ that represents how big of a step the spotted hyena takes when attacking its prey, in order to get the best optimal solution. The formula for attacking prey is expressed as,

$$\vec{X}(t+1) = \frac{\overrightarrow{C_h}}{N} \quad (21)$$

This spotted hyena optimizer is employed to tune the PI parameters to produce optimal results.

3. **Spotted Hyena Optimized PI Controller:** The SHO technique was used in this work to identify the PI controller's best attributes to improve the converter's dynamics. It is based on minimizing both inaccuracy in the inductor current measured sequentially, which are the inductor current peaks, and between the measured value and the reference voltage in steady state. The proposed objective function is shown in Equation (22).

$$F(t) = w_1F_1 + w_2F_2 \quad (22)$$

$$F_1 = \sqrt{\frac{\sum_i^N (P_i - \mu)^2}{N}} \quad (23)$$

$$F_2 \int_{t_o}^{t_f} |\varepsilon(t)|\, dt \quad (24)$$

Where F_2 stands for the Integral Absolute Error (IAE), and F_1 is the inductor current value's standard deviation, as recorded at every switch- opening moment.

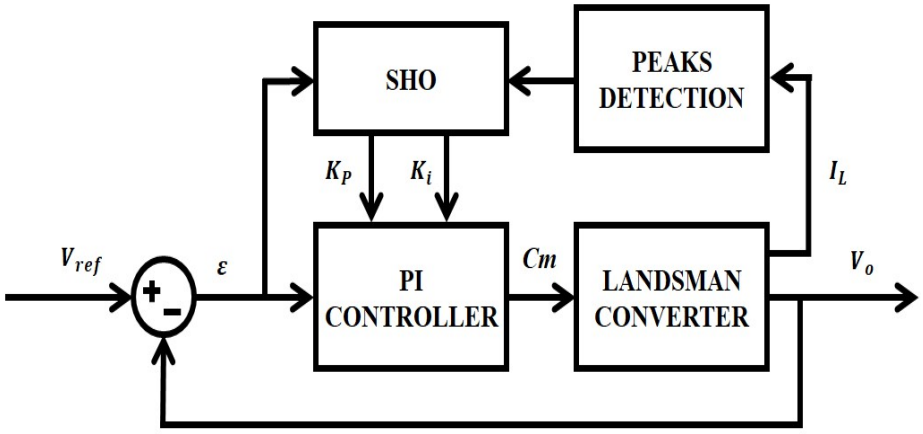

Figure 5: Closed Loop System with SHO

Figure 5 shows the system's control block diagram, where $K_p and\ K_i$ represent the proportional and integral gains that the SHO has achieved.

V. RESULTS AND DISCUSSION

This work develops the suggested technique for supplying high power applications with continuous power. The system is designed, modeled, and simulated under random and instant variation of irradiance. The experimental verification is carried out utilizing Matlab simulation to verify the suggested system. The suggested framework comprises of PV system, converter, and optimized PI controller. To improve the power supply to the grid with maintained stability under a range of situations, including partial shadowing and temperature changes, the system uses effective converter and control algorithm techniques. The parameter specification is listed in table 1.

Table 1: Parameter Specification

PV Panel	
No. of panels	20 panels
Peak power	10kW
Open circuit voltage	22.6V
Short circuit voltage	12V
No. of PV cells	36
Landsman Converter	
C_f	$4.7\mu F$
C_1	$4.7\mu F$
L_f	1mH
L_O	1mH
L_{in}	1mH

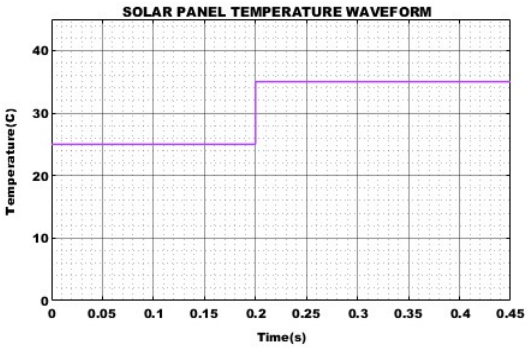

Figure 6: (a) Temperature wave form

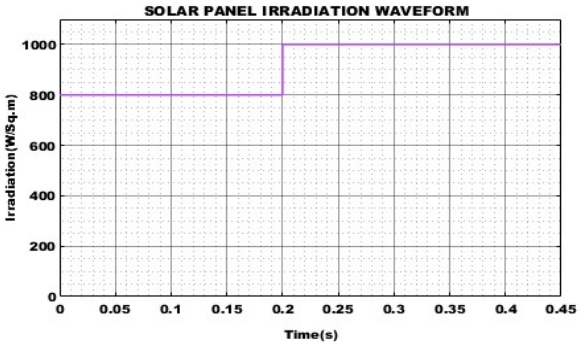

Figure 6: (b) Irradiation wave form

Figure 6(a) and 6(b) represents the temperature and irradiation waveform respectively. In figure 6(b) the PV system is observed by changing the irradiance level from $800W/M^2$ to $1000\,W/M^2$ and the temperature waveform represented in figure 6(a) indicates that the temperature shows the variation from $25^oC\ to\ 35^oC$ at 0.2s.

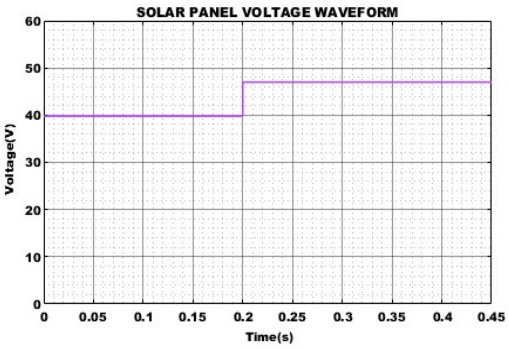

Figure 7: (a) Voltage waveform of solar panel

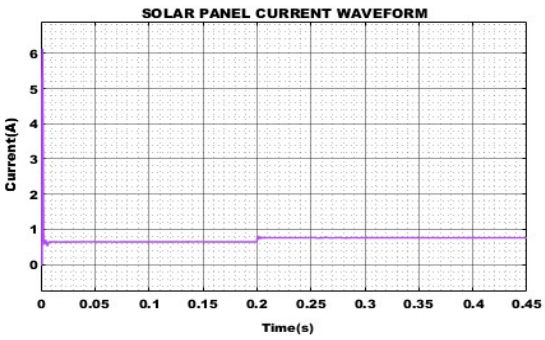

Figure 7: (b) Current wave form of solar panel

The solar panel's output current and voltage waveform are displayed correctly in Figures 7(a) and 7(b). Variable solar PV conditions cause the output power to fluctuate. As a result, a Landsman converter and spotted hyena-optimized PI controller are used to supply stable current to the grid even in the presence of dynamic conditions. The photovoltaic cell's resulting voltage is maintained despite changes in irradiance caused by external factors, as it is seen from the graph above.

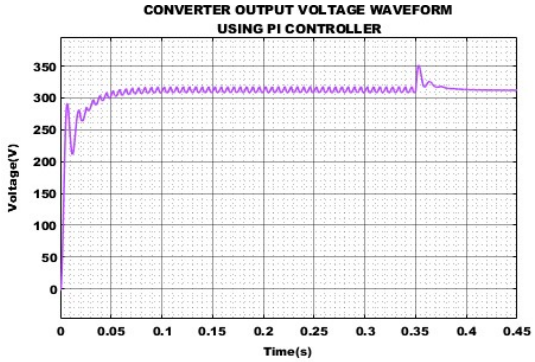

Figure 8: (a) voltage waveform of converter Output using PI controller output

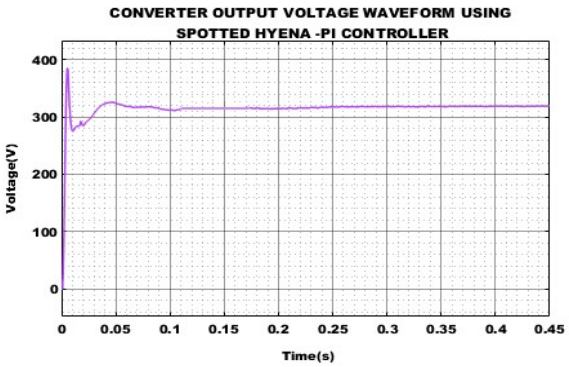

Figure 8: (b) Voltage waveform of converter using spotted Hyena PI Controller

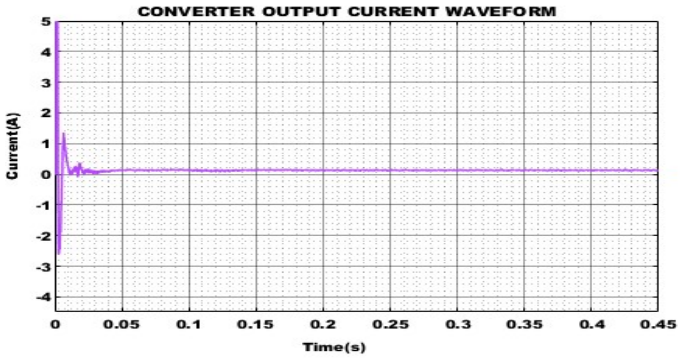

Figure 8: (c) Converter Output Current Waveform

Converter output waveform using PI controller and spotted hyena PI controller is represented in figure 8(a) and 8(b) respectively. The figure shows that the output voltage is not kept steady when using a PI controller. Figures 8(b) and 8(c) accordingly indicate how the output voltage and current are kept stable using Spotted Hyena optimized PI controller.

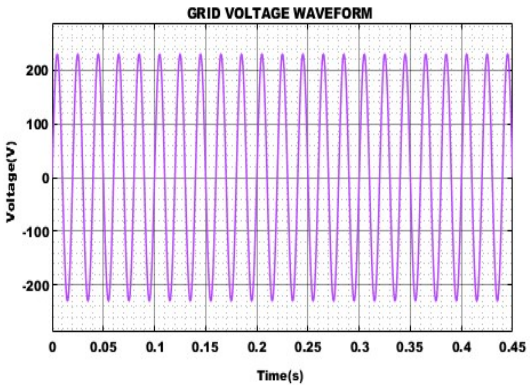

Figure 9: (a) Waveform of Grid Voltage

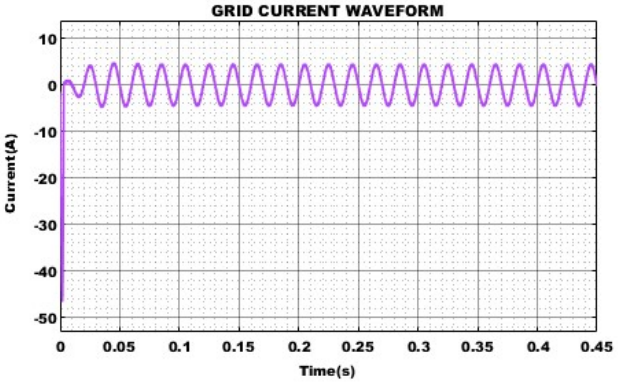

Figure 9: (b) Waveform of grid Current

Figures 9(a) and 9(b) correspondingly illustrate the grid voltage and current waveform. By obtaining a pure sine wave devoid of any harmonics, a low THD value of grid current is achieved.

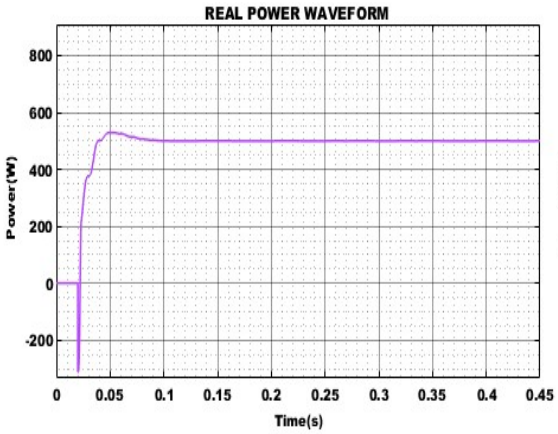

Figure 10: (A) Waveform of Real Power

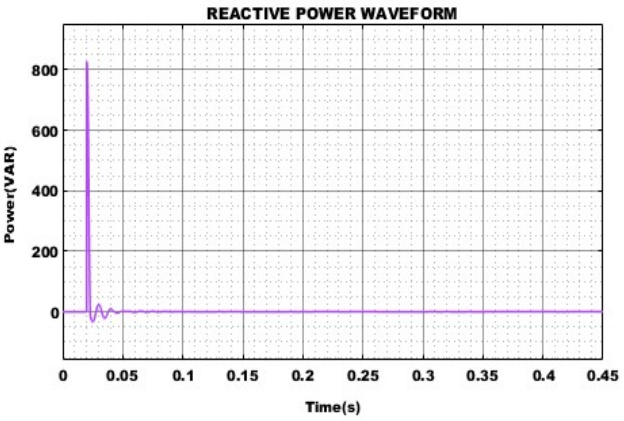

Figure 10: (b) Waveform of Reactive Power

Figure 10(a) and 10(b) shows the reactive and actual power waveforms. The real power is measured to be 500W, whereas the reactive power is modest. In this case, the PV connected grid system benefits from controlled and limited reactive power consumption since it allows for efficient utilization of available power resources.

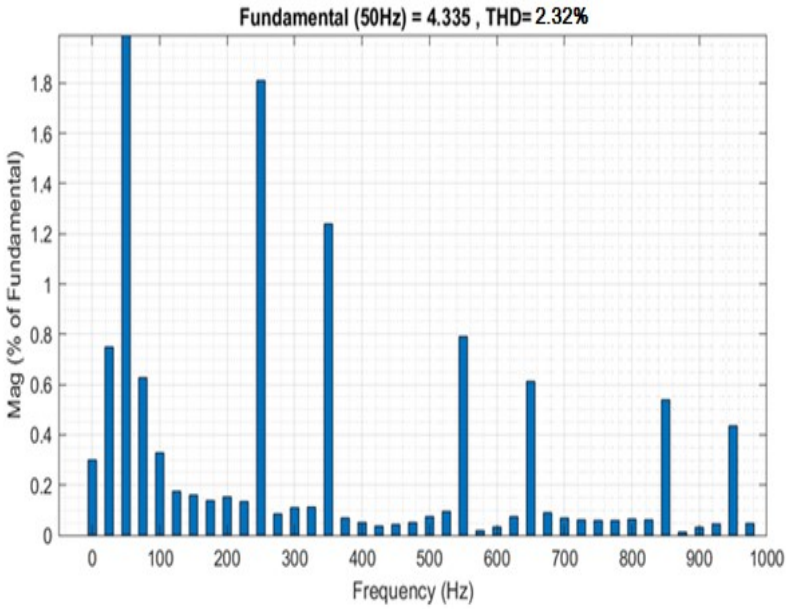

Figure 11: Total Harmonic Distortion (THD)

The THD graph is represented in figure 11. From the graph, it is observed that the low THD value is achieved which is of 2.32%. By attaining the low THD, high power factor and high-power efficiency is achieved. The THD comparison graph is shown in figure 12. It shows that the Landman converter achieves less harmonic distortion compared to other converters.

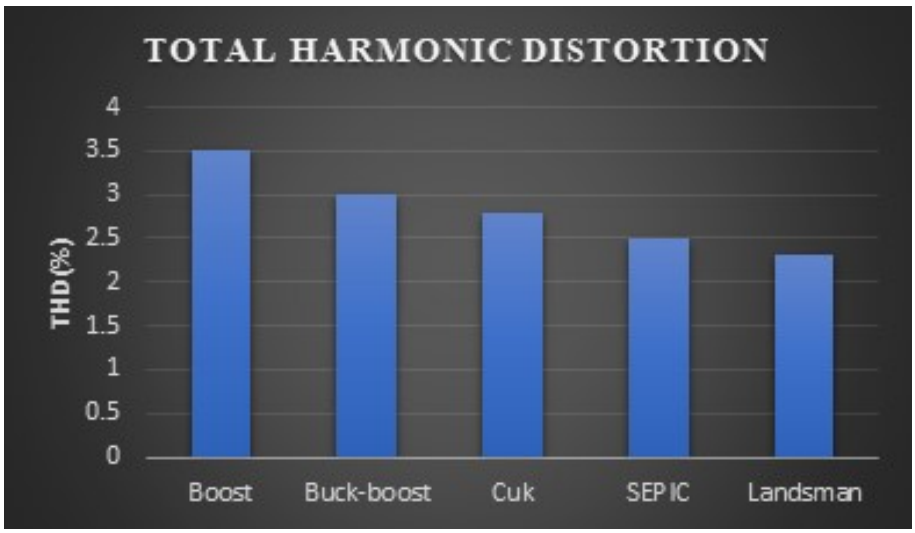

Figure 12: Comparison of Total Harmonic Distortion

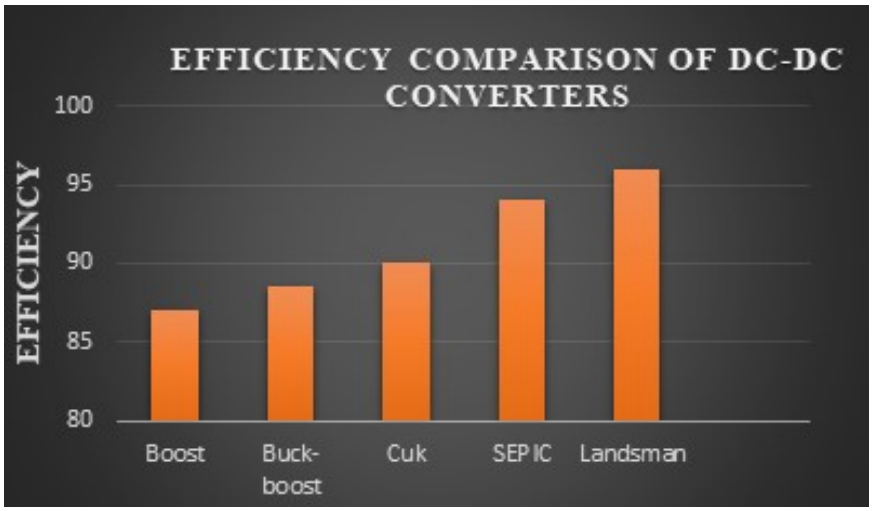

Figure 13: Comparison of Efficiency with Different Converters

Figure 13 illustrates a comparison of effectiveness with several converters and shows that the landsman converter gets an impressive efficiency of 96% when compared with various converters such the boost, Buck-boost, Cuk, and SEPIC converter.

VI. CONCLUSION

In this work, PV tied grid application utilizing Landsman DC-DC converter with the spotted hyena optimized PI controller has been proposed, examined and validated. The proposed system's layout and operation in Continuous Conduction Mode provided the advantages of high voltage gain and decreased input and output current ripples caused by inductors in the converter's input and output. The trial findings under dynamic conditions are validated to find the execution of the proposed system. The outcomes show that the effectiveness of the proposed approach meets the criteria for enhanced power quality based grid-tied PV applications. In addition, a high efficiency of 96% is attained while the THD of the input current is decreased to 2.32%. As a result, the suggested converter with efficient optimization-based PI controller intends to be a cost-effective, dependable, and acceptable replacement for the standard lossy and inefficient DC-DC converter.

REFERENCE

[1] Iram Akhtar, Sheeraz Kirmani, Mohammed Jameel 2021, “Reliability Assessment of Power System Considering the Impact of Renewable Energy Sources Integration Into Grid With Advanced Intelligent Strategies”, IEEE Access, vol. 9, no. 2, pp. 32485-32497.
[2] M. Arjun, Vanjari Venkata Ramana, Roopa Viswadev, B. Venkatesaperumal 2019, “Small Signal Model for PV Fed Boost Converter in Continuous and Discontinuous Conduction Modes”, IEEE Transactions on Circuits and Systems II: Express Briefs, vol. 66, no.7, pp. 1192-1196.
[3] Kumaran Nathan, Saikat Ghosh, Yam Siwakoti, Teng Long 2019, “A New DC–DC Converter for Photovoltaic Systems: Coupled-Inductors Combined Cuk-SEPIC Converter”, IEEE Transactions on Energy Conversion, vol.34, no. 3, pp. 191-201.
[4] Keyvan Yari, Hamed Mojallali, S. Hamid Shahalami 2022, “A New Coupled-Inductor-Based Buck–Boost DC–DC Converter for PV Applications”, IEEE Transactions on Power Electronics, vol. 37, no. 1, pp. 687-699.

[5] Gautam A. Raiker, Umanand Loganathan 2021, "Current Control of Boost Converter for PV Interface With Momentum-Based Perturb and Observe MPPT", IEEE Transactions on Industry Applications, vol. 7,no. 4, pp. 4071-4079.
[6] Mohammed Alsumiri 2019, "Residual Incremental Conductance Based Nonparametric MPPT Control for Solar Photovoltaic Energy Conversion System", IEEE Access, vol. 7, no. 6, pp. 4071-4079.
[7] Nabil Farah, Md. Hairul Nizam Talib, Nor Shahida Mohd Shah, Qazwan Abdullah, Zulkifilie Ibrahim, Jurifa Binti Mat Lazi, Auzani Jidin 2019, "A Novel Self-Tuning Fuzzy Logic Controller Based Induction Motor Drive System: An Experimental Approach", IEEE Access, vol. 7, no. 5, pp. 68172-68184.
[8] Alper Nabi Akpolat, Mohammad Reza Habibi, Hamid Reza Baghaee, Erkan Dursun, Ahmet Emin Kuzucuoğlu, Yongheng Yang, Tomislav Dragičević, Frede Blaabjerg 2022, "Dynamic Stabilization of DC Microgrids Using ANN-Based Model Predictive Control", IEEE Transactions on Energy Conversion, vol. 37, no.2, pp. 999-1010.
[9] Evren Isen 2022, "Determination of Different Types of Controller Parameters Using Metaheuristic Optimization Algorithms for Buck Converter Systems", IEEE Access, vol. 10, no. 12, pp. 127984-127995.
[10] Bruno Leandro Galvão Costa, Vinícius Dário Bacon, Sérgio A. Oliveira da Silva, Bruno Augusto Angélico 2017, "Tuning of a PI-MR Controller Based on Differential Evolution Metaheuristic Applied to the Current Control Loop of a Shunt-APF", IEEE Transactions on Industrial Electronics, vol. 64, no. 6, pp. 4751-4761.
[11] Jaime W. Zapata, Samir Kouro, Gonzalo Carrasco, Hugues Renaudineau, Thierry A. Meynard 2019, "Analysis of Partial Power DC–DC Converters for Two-Stage Photovoltaic Systems",IEEE Journal of Emerging and Selected Topics in Power Electronics, vol. 55, no. 6, pp. 7442-7451.
[12] Rui Li, Fangyuan Shi 2019, "Control and Optimization of Residential Photovoltaic Power Generation System with High Efficiency Isolated Bidirectional DC–DC Converter", IEEE Access, vol. 7, no. 8, pp. 116107-116122.
[13] Pierre Le Métayer, Quentin Loeuillet, François Wallart, Cyril Buttay, Drazen Dujic, Piotr Dworakowski 2023, "Phase-Shifted Full Bridge DC–DC Converter for Photovoltaic MVDC Power Collection Networks", IEEE Access, vol. 11, no. 2, pp. 19039-19048.
[14] Ali M. Eltamaly, M. S. Al-Saud, Ahmed G. Abokhalil 2019, "A Novel Bat Algorithm Strategy for Maximum Power Point Tracker of Photovoltaic Energy Systems Under Dynamic Partial Shading", IEEE Access, vol. 8, no. 1, pp. 10048-10060.
[15] Moustafa Adly, Kai Strunz 2019, "Efficient Digital Control for MPP Tracking and Output Voltage Regulation of Partially Shaded PV Modules in DC Bus and DC Microgrid Systems", IEEE Transactions on Power Electronics, vol.34, no. 7, pp. 6309-6319.

